UNIVERSITY OF LEEDS

This is a repository copy of *Comparison of AC Optimal Power Flow Methods in Low-Voltage Distribution Networks*.

White Rose Research Online URL for this paper:
https://eprints.whiterose.ac.uk/178191/

Version: Accepted Version

eprints@whiterose.ac.uk
https://eprints.whiterose.ac.uk/

Comparison of AC Optimal Power Flow Methods in Low-Voltage Distribution Networks

Agnes M. Nakiganda
Dept. of Electronic & Electrical Eng.
University of Leeds, UK
el14amn@leeds.ac.uk

Shahab Dehghan
Dept. of Electrical & Electronic Eng.
Imperial College London, UK
s.dehghan@imperial.ac.uk

Petros Aristidou
Dept. of Elec. & Comp Eng. & Informatics
Cyprus University of Technology, Cyprus
petros.aristidou@cut.ac.cy

Abstract—Embedded with producers, consumers, and pro-sumers, active Low-Voltage Distribution Networks (LVDNs) with bi-directional power flows are rising to over-shadow the investment and operation planning in power systems. The Optimal Power Flow (OPF) has been extensively used in the recent years to solve different investment and operation planning problems in LVDNs. However, OPF is inherently a complex non-linear and non-convex optimization problem. Hence, different linearization and convexification models have been introduced in the literature to enhance the modeling accuracy and computational tractability of the OPF problem in LVDNs. In this paper, five multi-period OPF models (including the basic non-linear and non-convex one) are presented, with different linearizations/convexifications for the power flow equations. The proposed models are implemented on the IEEE 34-bus test system and their modeling accuracy and computational complexity are compared and discussed.

Index Terms—Convex Optimization, Distribution Networks, Exact Conic Relaxation, Multi-Period Optimal Power Flow.

I. Introduction

In the past, distribution grids were modeled as passive elements or aggregated loads, due to their lack of participation in power, frequency and voltage control. In recent years, the electricity grid has seen major changes in the design and operation of Low Voltage (LV) Distribution Networks (DNs) due to the proliferation of Distributed Energy Resources (DERs), mainly consisting of Renewable Energy Sources (RES), and the requirement for them to provide active support to the grid. The electricity grid has become less reliant on generation and control from the bulk conventional units and more dependent on diverse DERs located in DNs. This emergence of Active Distribution Networks (ADNs) and their increased impact to the grid, requires more accurate DN modeling, both in investment and operation planning problems.

One of the major tools used for investment and operation planning in power systems is the Optimal Power Flow (OPF) [1], which aims at obtaining a feasible and optimal operating point that satisfies operational and physical constraints at the minimum cost. However, OPF is a complex problem due to the non-linear and non-convex nature of the AC power flow equations that govern the grid's physical laws. In finding the solution to an OPF problem, the challenge thus lies between AC feasibility (i.e., exactness), global optimality, and computational efficiency of the model adopted.

In the past, different optimization techniques with various linearizations, convexifications, and approximations have been proposed to obtain locally or globally optimal solutions of the OPF problem under specific assumptions [2]. In general, non-linear and non-convex techniques converge to locally optimal solutions with no guarantees on global optimality, while their optimal solutions exactly satisfy the original power flow equations. In contrast, convex relaxations provide a lower bound on the objective, yield a global optimum, can certify the existence of problem infeasibility and tend to be tractable [2]–[4]. However, the solution obtained is not always physically meaningful and thus can be inapplicable practically [3], [5].

In this study, we analyze five different widely adopted OPF formulations used in ADNs and microgrids under different performance metrics. These OPF models include basic Non-Linear OPF [6], DistFlow (DF) [7], [8], Linearized DistFlow (LinDF) [9] without line shunts, Extended DistFlow (ExDF) with line shunts [7], and Extended Augmented DistFlow (ExAgDF) [8]. Our focus is to study their performance in practical situations based on metrics defining the optimality gap and normalized distance to a local AC feasible solution. Additionally, we evaluate their computational performance in a multi-period optimization problem with varying load and generation profiles for the IEEE 34-bus test system, thus analyzing their applicability for adoption in LV networks.

The rest of the paper is organized as follows. In Section II, the mathematical formulations of the five AC OPF models mentioned above are presented. Section III presents the metrics used to compare the different formulations. In Section IV, the proposed OPF models are implemented on the IEEE 34-bus test system and their performances are evaluated and discussed. Finally, in Section V, the main conclusions of the paper are summarized.

II. Optimal power flow problem formulations

A. Notations

Let $\mathbf{j} = \sqrt{-1}$, $|\bullet|$ denote the magnitude, $\bullet^*$ complex conjugate while $\underline{\bullet}/\overline{\bullet}$ represent lower/upper bounds of the quantity $\bullet$. In this study, we consider a balanced radial DN composed of nodes $i \in \mathcal{N}$, with index 1 defined as the Point of Common Coupling (PCC). The active and reactive power injections at each bus i are defined by $s_i = p_i + \mathbf{j}q_i$. The power injections are derived from the bulk grid import (export), DERs, and loads defined by: s^{imp} (s^{exp}), s_g : $g \in \mathcal{G}$ and s_i^{d}, respectively. Set $\mathcal{G}^i$ represents all generators connected to node i. The voltage at each bus is defined by $V_i = |V_i| \angle \theta_i$ with the square of voltage magnitude denoted by $v_i = |V_i|^2$. Bus voltage
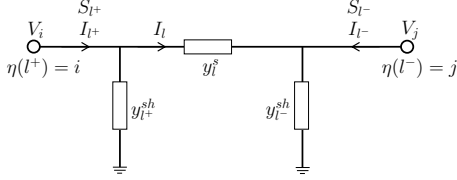
Fig. 1. The Π model of the line and notation used in OPF formulation.

at the PCC node is fixed at $V_1 = 1\angle 0°$ pu. Each branch $l \in \mathcal{L}$ is represented by a Π model (Fig. 1) with the sending and receiving ends denoted by l^+ and l^-, respectively, connected by two adjacent nodes $\eta(l^+) = i$ and $\eta(l^-) = j$. Set $\mathcal{L}^{\eta(l^+)}$ includes all lines connecting from downstream of a node/line in the *from* direction indexed by m, while $\mathcal{L}^{\eta(l^-)}$ includes all lines connecting from upstream in the *to* direction indexed by n. y_l^s is the series admittance given by $y_l^s = g_l + \mathbf{j}b_l = 1/(r_l + \mathbf{j}x_l) = 1/z_l$ while $y_{l^+}^{sh} = \mathbf{j}b_{l^+}^{sh}$ and $y_{l^-}^{sh} = \mathbf{j}b_{l^-}^{sh}$ are the shunt admittances at the sending and receiving ends, respectively ($y_{l^+}^{sh} = y_{l^-}^{sh} = \mathbf{j}b_l^{sh}/2$). The active and reactive power flows into the line at the sending (receiving) end are denoted by $S_{l^+} = P_{l^+} + \mathbf{j}Q_{l^+}$ ($S_{l^-} = P_{l^-} + \mathbf{j}Q_{l^-}$). $I_{l^+} = |I_{l^+}|\angle\vartheta_{l^+}$ ($I_{l^-} = |I_{l^-}|\angle\vartheta_{l^-}$) is the current flowing into the line from sending (receiving) nodes while I_l is the current in the longitudinal section. The square of current flow is denoted by $f_{l^+} = |I_{l^+}|^2$, $f_{l^-} = |I_{l^-}|^2$, and $f_l = |I_l|^2$ in each case. Each time step in the planning horizon T is indexed by $t \in \mathcal{T}$.

B. Non-Convex Extended AC Optimal Power Flow

Usually, the OPF problem seeks to minimize power generation costs and power losses, or maximize power reserves, subject to power balance constraints and operational limits. The compact formulation of this problem can be defined as:

$$\underset{\chi}{\textbf{minimize}} : \Theta(\chi) \tag{1a}$$

$$\textbf{subject to} : h_k(\chi) = 0, \ k = 1, \ldots, n, \tag{1b}$$

$$g_k(\chi) \le 0, \ k = 1, \ldots, m \tag{1c}$$

where χ represents the operational decision variables that include: voltages, power in-feed of different generators, power flows and power consumption in the network.

In (1a) is the objective function, (1b) defines the AC power flow equations while the operational limits on the control variables are defined in (1c). In the following, we present different formulations of (1b) and (1c) considering the same objective function in each case defined by:

$$\Theta = \min_{\chi} \left(\sum_{t \in \mathcal{T}} \left(C^{\text{imp}}p_t^{\text{imp}} - C^{\text{exp}}p_t^{\text{exp}} \right) + \sum_{t \in \mathcal{T}} \sum_{g \in \mathcal{G}} C^{\text{g}}p_{gt} \right.$$
$$\left. + \sum_{t \in \mathcal{T}} \sum_{l \in \mathcal{L}} C^{\text{loss}}p_{lt}^{\text{loss}} \right) \tag{2}$$

where χ defines the decision variables while p^{loss} is the active power loss function for the algorithm. The objective is to minimize the generation costs and the network real power losses.

In **Model 1** the non-linear AC OPF formulation is presented taking into account the line shunts. In (3a), the power balance at each node in the network is enforced while constraints (3b)-(3d) define the active and reactive power flows at both ends of each line. In (3e)-(3f), the thermal line limits are enforced while constraint (3g) ensures that voltage

---

Model 1 : Generic AC Optimal Power Flow [6]

$$s_{it}^{\text{d}} - s_{t|i=1}^{\text{imp}} + s_{t|i=1}^{\text{exp}} - \sum_{g \in \mathcal{G}^i} s_{gt}$$
$$= \sum_{\eta(l^+)=i} S_{l^+} + \sum_{\eta(l^-)=i} S_{l^-} \qquad \forall it \tag{3a}$$

$$S_{l^+} = V_{\eta(l^+)t}(I_{l^+})^*, \qquad S_{l^-} = V_{\eta(l^-)t}(I_{l^-})^*, \qquad \forall lt \tag{3b}$$

$$I_{l^+} = y_l^s(V_{\eta(l^+)} - V_{\eta(l^-)}) + y_{l^+}^{sh}V_{\eta(l^+)}, \qquad \forall lt \tag{3c}$$

$$I_{l^-} = y_l^s(V_{\eta(l^-)} - V_{\eta(l^+)}) + y_{l^-}^{sh}V_{\eta(l^-)}, \qquad \forall lt \tag{3d}$$

$$|S_{l^+}| \le \overline{S}_l \quad \text{or} \quad |I_{l^+}| \le \overline{I}_l, \qquad \forall lt \tag{3e}$$

$$|S_{l^-}| \le \overline{S}_l \quad \text{or} \quad |I_{l^-}| \le \overline{I}_l, \qquad \forall lt \tag{3f}$$

$$\underline{V} \le |V_{\eta(l)t}| \le \overline{V}, \qquad |V_{t|\eta(l)=1}| = 1, \ \theta_{t|\eta(l)=1} = 0, \qquad \forall it \tag{3g}$$

$$0 \le p_t^{\text{imp}} \le \overline{p}_t^{\text{imp}}, \qquad 0 \le p_t^{\text{exp}} \le \overline{p}_t^{\text{exp}} \qquad \forall it \tag{3h}$$

$$0 \le q_t^{\text{imp}} \le \overline{q}_t^{\text{imp}}, \qquad 0 \le q_t^{\text{exp}} \le \overline{q}_t^{\text{exp}} \qquad \forall it \tag{3i}$$

$$\underline{p}_{gt} \le p_{gt} \le \overline{p}_{gt}, \qquad \underline{q}_{gt} \le q_{gt} \le \overline{q}_{gt} \qquad \forall gt \tag{3j}$$

$$\underline{p}_{it}^{\text{d}} \le p_{it}^{\text{d}} \le \overline{p}_{it}^{\text{d}}, \qquad \underline{q}_{it}^{\text{d}} \le q_{it}^{\text{d}} \le \overline{q}_{it}^{\text{d}} \qquad \forall it \tag{3k}$$

---

magnitudes are kept within limits and voltage reference for the PCC node $\eta(l) = 1$ is set in (3g). The limitations on power imported (resp. exported) from (resp. to) the grid as well as power provided by the distributed generators and load demand are defined in (3h)-(3k).

Note that due to the non-linearity of the power flow equations in (3b)-(3d), this non-convex model can be solved only through the adoption of non-linear programming (NLP) techniques. Given that the model converges, the solution is locally optimal with no guarantees on global optimality.

C. Branch Flow Model with Approximations and Relaxations

Convex relations yield global optimal bounds to the original non-convex AC OPF. The exactness of the relaxation will depend on the tightness of the envelope and defined sufficient conditions thus providing a lower bound on the objective at the least. In practical applications, however, sufficient conditions may not always be entirely satisfied [10]. In this study, we focus on formulations that adopt the Branch Flow Model (BFM) due to its desirable numerical characteristics in relation to radial networks [11]. This model formulates the power flow equations in terms of active and reactive power flows, squared current magnitude flows and squared voltage magnitude at each node as indicated in [11].

At the core of the BFM relaxations based on Second-Order Cone Programming (SOCP), two relaxation steps are followed: (i) voltage and current angles are eliminated from the branch flow equations, and (ii) quadratic equality power flow equations are relaxed into inequality constraints [11].

Model 2 presents the DistFlow model where the AC power flows are described by constraints (4a)-(4e). Constraint (4d) defines the SOCP relaxation applied to the equality constraint in the original model thus resulting in the convexification of the model. The model can be used with both zero (DF) and non-zero line shunts (DF$_{w/s}$) by modification of line parameter b_l^{sh}. The sufficient conditions for the exactness of this model are defined in [10] for the case of zero line shunts.

A modified linear approximation of the DistFlow formulation in **Model 2** defined as LinDistFlow is presented in **Model 3**. Here, the power flow equations are defined as in (5a)-(5b) with the assumption that line losses indicated by the

Model 2 : Adapted DistFlow Relaxation ($\text{DF}_{w/s}$) [7], [8]

$$S_{tl+} = s^{\text{d}}_{t\eta(l-)} - s^{\text{imp}}_{t|\eta(l-)=1} + s^{\text{exp}}_{t|\eta(l-)=1} - \sum_{g \in \mathcal{G}^{\eta(l-)}} s_{gt} +$$

$$\sum_{m \in \mathcal{L}^{\eta(l+)}} S_{tl^+_m} + z_l f_{lt} - \mathbf{j}(v_{\eta(l+)t} + v_{\eta(l-)t}) \frac{b^{sh}_l}{2}, \quad \forall lt \quad (4a)$$

$$S_{tl+} = s^{\text{d}}_{t\eta(l-)} - s^{\text{imp}}_{t|\eta(l-)=1} + s^{\text{exp}}_{t|\eta(l-)=1} - \sum_{g \in \mathcal{G}^{\eta(l-)}} s_{gt}$$

$$+ \sum_{m \in \mathcal{L}^{\eta(l+)}} S_{tl^+_m}, \quad \forall lt \quad (4b)$$

$$v_{\eta(l-)t} = v_{\eta(l+)t} + |z_l|^2 f_{lt}$$

$$- 2 \text{Re}\left(z_l^* \left(S_{tl+} + \mathbf{j} v_{\eta(l+)t} \frac{b^{sh}_l}{2} \right) \right), \quad \forall lt \quad (4c)$$

$$f_{lt} \geq \frac{|S_{tl+} + \mathbf{j} v_{\eta(l+)t} \frac{b^{sh}_l}{2}|^2}{v_{\eta(l+)t}} \text{ or } \frac{|S_{tl-} - \mathbf{j} v_{\eta(l-)t} \frac{b^{sh}_l}{2}|^2}{v_{\eta(l-)t}}, \quad \forall lt \quad (4d)$$

$$\overline{f}_l v_{\eta(l+)t} \geq |S_{tl+}|^2, \quad \overline{f}_l v_{\eta(l-)t} \geq |S_{tl-}|^2, \quad \forall lt \quad (4e)$$

$$|S_{l+}| \leq \overline{S}_l, \quad |S_{l-}| \leq \overline{S}_l, \quad \forall lt \quad (4f)$$

$$\underline{v} \leq v_{\eta(l)t} \leq \overline{v}, \quad v_{t\eta(l)=1} = 1, \quad \forall it \quad (4g)$$

$$(3h) - (3k) \quad (4h)$$

Model 3 : Modified Lin-DistFlow Relaxation (LinDF) [9]

$$S_{tl+} + s_{t\eta(l-)} = \sum_{m \in \mathcal{L}^{\eta(l+)}} S_{tl^+_m}, \quad \forall lt \quad (5a)$$

$$v_{\eta(l-)t} = v_{\eta(l+)t} - 2\left(r_l P_{tl+} + x_l Q_{tl+} \right), \quad \forall lt \quad (5b)$$

$$- \overline{S}_l \leq P_{tl+} + a_d Q_{tl+} \leq \overline{S}_l, \quad \forall lt \quad (5c)$$

$$- \overline{S}_l \leq P_{tl+} - a_d Q_{tl+} \leq \overline{S}_l, \quad \forall lt \quad (5d)$$

$$- \overline{S}_l \leq a_d P_{tl+} + Q_{tl+} \leq \overline{S}_l, \quad \forall lt \quad (5e)$$

$$- \overline{S}_l \leq a_d P_{tl+} - Q_{tl+} \leq \overline{S}_l, \quad \forall lt \quad (5f)$$

$$(3g) - (3k) \quad (5g)$$

---

square of current flow are negligible in comparison with the active and reactive power flows (i.e., $f_{lt} << S_{tl} \therefore f_{lt} \simeq 0$) [9]. A modification [9] to include line flow limits using constraints (5c)-(5f) is made. These are linear approximations of the quadratic line flow limit (3e) obtained by inner approximations of the thermal loading circle [12]. Parameter a_d is the derivative of the lines constructing the segments of the convex approximation. This model provides an upper bound on voltage and lower bound on power flows in the network [9].

Model 4 presents a variant of BFM relaxation for the AC power flows considering non-zero line shunts [7]. Note that unlike **Model 2** where current flow is only defined in the longitudinal section of the Π model in Fig. 1, the current and power flows here are defined at both ends of the line. This enhances the non-violation of the line ampacity limits in the physical network [6]. Here, (6a)-(6e) define the power flow equations while the line flows are constrained by (6f). Parameter α_{l+} is defined as $\alpha_{l+} = 1 + z_l y^{sh}_{l+}$. Constraint (6b) has been relaxed from an equality to inequality thus obtaining an SOCP relaxation of the non-convex power flow. Sufficient conditions for the exact SOCP relation of this model are detailed in [7].

The formulation in **Model 2** is modified by adding a new set of constraints as indicated in (7c)-(7m) to obtain an augmented relaxation of the OPF problem defined by **Model 5** [8]. The augmentations create inner approximations

---

Model 4 : Extended DistFlow Relaxation with Line Shunts (ExDF) [7]

$$s_{it} = \sum_{\eta(l+)=i} S_{l+} + \sum_{\eta(l-)=i} S_{l-} \quad \forall it \quad (6a)$$

$$f_{tl+} v_{\eta(l+)} \geq |S_{tl+}|^2 \text{ or } f_{tl-} v_{\eta(l-)} \geq |S_{tl-}|^2, \quad \forall lt \quad (6b)$$

$$|\alpha_{l+}|^2 v_{t\eta(l+)} - v_{t\eta(l-)} = 2 \text{Re}(\alpha_{l+} z_l^* S_{tl+}) - |z_l|^2 f_{tl+}, \quad \forall lt \quad (6c)$$

$$|\alpha_{l-}|^2 v_{t\eta(l-)} - v_{t\eta(l+)} = 2 \text{Re}(\alpha_{l-} z_l^* S_{tl-}) - |z_l|^2 f_{tl-}, \quad \forall lt \quad (6d)$$

$$\alpha_{l+}^* v_{t\eta(l+)} - z_l^* S_{tl+} = \left(\alpha_{l-}^* v_{t\eta(l-)} - z_l^* S_{tl-} \right)^*, \quad \forall lt \quad (6e)$$

$$0 \leq f_{l+} \leq (\overline{f}_l), \quad 0 \leq f_{l-} \leq (\overline{f}_l), \quad \forall lt \quad (6f)$$

$$\underline{v} \leq v_{\eta(l)t} \leq \overline{v}, \quad v_{t\eta(l)=1} = 1, \quad \forall it \quad (6g)$$

$$(3h) - (3k) \quad (6h)$$

(restrictions) for the feasible space of the problem that ensure a tighter envelope for the original relaxation in **Model 2**. This is achieved by introducing auxiliary variables on the lines and node voltages that apply security constraints on these variables. In **Model 5**, auxiliary variables defined by superscripts $\hat{\bullet}/\check{\bullet}$ indicate the lower/upper bound on the associated variable. Note that while the set of security constraints improves the feasibility of the model, it creates a larger set of optimization variables that widens the solution space. Sufficient conditions for this relaxation are detailed in [8].

III. MODEL FEASIBILITY ASSESSMENT

A relaxed OPF model is "exact" if its optimal solution satisfies the original non-convex AC power flow equations. In the following, we evaluate the optimality, tractablity, and exactness of the solution to the OPF problem provided by each model. The metrics used in assessment of a model performance include the following.

A. Optimality gap

This metric compares the quality of the optimal solution for approximated/relaxed models (Θ^{relax}) w.r.t the optimal solution of the basic non-convex NLP-based OPF model (Θ^{NLP}). It is defined as:

$$\text{OG}^{\text{relax}} = \left| \frac{\Theta^{\text{NLP}} - \Theta^{\text{relax}}}{\Theta^{\text{NLP}}} \right| \quad (8)$$

B. Average normalized deviation from NLP

This metric compares the divergence of the optimal value of decision variable $\chi^{\text{relax}}_\bullet$ obtained for the approximated/relaxed models w.r.t. the optimal solution $\chi^{\text{NLP}}_\bullet$ obtained from the NLP model. It provides an indication of the AC feasibility of the solutions of the approximations/relaxations for each of the variables and is defined as follows:

$$\delta^{\text{relax}}_\chi = \frac{1}{|\mathcal{T}| \times |\Omega|} \sum_{t \in \mathcal{T}} \sum_{n \in \Omega} \left| \frac{\chi^{\text{NLP}}_{nt} - \chi^{\text{relax}}_{nt}}{\chi^{\text{NLP}}_{nt}} \right| \quad (9)$$

The sets $\mathcal{T}$ and Ω are the corresponding sets where variable $\chi_\bullet \equiv \chi_{nt}$ lies.

IV. SIMULATION AND RESULTS

A. System Description

We evaluate the aforementioned five OPF models on a modified version of the IEEE 34-bus network [13]. The system is adjusted to be balanced and include four distributed Photo-Voltaic (PV) units. The parameters for the network are

Model 5 : Augmented DistFlow with Line Shunts (ExAgDF) [8]

$$(4a) - (4e) \tag{7a}$$

$$(3h) - (3k) \tag{7b}$$

$$\hat{S}_{tl+} + s_{t\eta(l-)} = \sum_{m \in \mathcal{L}^{\eta(l+)}} \hat{S}_{tl_m^+} - \mathbf{j} \left(\check{v}_{\eta(l+)t} + \check{v}_{\eta(l-)t} \right) \frac{b_l^{sh}}{2}, \qquad \forall lt \tag{7c}$$

$$\hat{S}_{tl-} + s_{t\eta(l-)} = \sum_{m \in \mathcal{L}^{\eta(l+)}} \hat{S}_{tl_m^+}, \qquad \forall lt \tag{7d}$$

$$\check{v}_{\eta(l-)t} = \check{v}_{\eta(l+)t} - 2 \operatorname{Re} \left(z_l^* \left(S_{tl+} + \mathbf{j} \check{v}_{\eta(l+)t} \frac{b_l^{sh}}{2} \right) \right), \ \forall lt \tag{7e}$$

$$\check{S}_{tl+} + s_{t\eta(l-)} = \sum_{m \in \mathcal{L}^{\eta(l+)}} \check{S}_{tl_m^+} + z_l \check{f}_{lt} - \mathbf{j}(v_{\eta(l+)t} + v_{\eta(l-)t}) \frac{b_l^{sh}}{2}, \quad \forall lt \tag{7f}$$

$$\check{S}_{tl-} + s_{t\eta(l-)} = \sum_{m \in \mathcal{L}^{\eta(l+)}} \check{S}_{tl_m^+}, \qquad \forall lt \tag{7g}$$

$$\check{f}_l v_{\eta(l+)t} \geq \max \left(\left| \hat{P}_{tl+} \right|^2, \left| \check{P}_{tl+} \right|^2 \right) + \max \left(\left| \hat{Q}_{tl+} + \check{v}_{\eta(l+)t} \frac{b_l^{sh}}{2} \right|^2, \left| \check{Q}_{tl+} + v_{\eta(l+)t} \frac{b_l^{sh}}{2} \right|^2 \right), \ \forall lt \tag{7h}$$

$$\check{f}_l v_{\eta(l-)t} \geq \max \left(\left| \hat{P}_{tl-} \right|^2, \left| \check{P}_{tl-} \right|^2 \right) + \max \left(\left| \hat{Q}_{tl-} - \check{v}_{\eta(l-)t} \frac{b_l^{sh}}{2} \right|^2, \left| \check{Q}_{tl-} - v_{\eta(l-)t} \frac{b_l^{sh}}{2} \right|^2 \right), \ \forall lt \tag{7i}$$

$$\overline{f}_l v_{\eta(l+)t} \geq \max \left(\left| \hat{P}_{tl+} \right|^2, \left| \check{P}_{tl+} \right|^2 \right) + \max \left(\left| \hat{Q}_{tl+} \right|^2, \left| \check{Q}_{tl+} \right|^2 \right), \qquad \forall lt \tag{7j}$$

$$\overline{f}_l v_{\eta(l-)t} \geq \max \left(\left| \hat{P}_{tl-} \right|^2, \left| \check{P}_{tl-} \right|^2 \right) + \max \left(\left| \hat{Q}_{tl-} \right|^2, \left| \check{Q}_{tl-} \right|^2 \right), \qquad \forall lt \tag{7k}$$

$$\underline{v} \leq v_{it}, \qquad \check{v}_{\eta(l-)t} \leq \overline{v}, \qquad v_{t|n=1} = 1, \qquad \forall it \tag{7l}$$

$$\hat{P}_{tl+} \leq \check{P}_{tl+} \leq \overline{P}_{l+}, \qquad \hat{Q}_{tl+} \leq \check{Q}_{tl+} \leq \overline{Q}_{l+}, \qquad \forall lt \tag{7m}$$

as indicated in [13] where all loads are modified as balanced three-phase ones and all transformers are modeled as lines with series resistance and inductance. The base values of apparent power and voltage magnitude are assumed to be 1 MVA and 24.9 kV, respectively. The load and PV generation profiles adopted from [14] in Texas during 2016 for a 24-hour period. The optimization model was implemented in PYOMO [15] and GUROBI [16] was employed as the convex solver while IPOPT [17] was adopted for the NLP problem.

B. Discussion of Results

1) Optimality gap: In Fig. 2, the quality of the objective value based on the metric $\mathrm{OG}^{\mathbf{relax}}$ in (8) is presented. While a larger gap of over 10% is recorded in the models that do not consider shunt parameters (DF and LinDF), a near to zero gap is obtained in the case of the more accurate models (ExDF and ExAgDF). Although both the 25th and 75th percentiles of the LinDF are closer to AC optimality as compared to DF, this may not necessarily be an indication to AC feasibility of the solution. This will be highlighted in
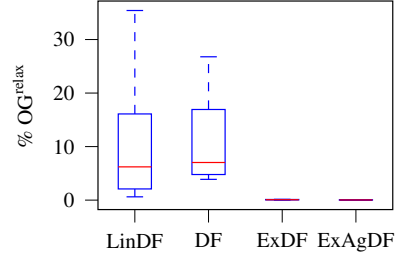

Fig. 2. Optimality gap of each model w.r.t the total operational cost of the AC NLP solution.

the the following where we look at the deviations of each of the variables to the local solution provided by the AC NLP model. Note that the LinDF model ignores the network losses thus providing an optimistic total cost in the objective.

2) Deviations from local optimality: A further study into the solutions provided by each model were made using the metric defined in (9). The voltage deviations are indicated in Fig. 3. The average deviations where recorded at 0.52%, 0.57%, 0.005% and 0.003% for the LinDF, DF, ExDF and ExAgDF models, respectively. The LinDF model marginally outperforms the DF model as its is known to provide an upper bound on voltage. This however is not the the case with regards to the line flow deviations presented in Fig. 4. The 75th percentile of the DF model is much lower than that of the LinDF model. The average deviations for active power line flows are obtained as 6.69%, 4.23%, 0.20% and 0.03% for the LinDF, DF, ExDF and ExAgDF models, respectively. The 75th percentile of the ExDF and ExAgDF models exhibit negligible deviations while the LinDF model shows the highest deviation. Note that this model neglects network losses thus providing a higher variation in line flow deviations. A similar trend is observed in Fig. 5 with regards to power injection deviations.

It is noteworthy to mention that ignoring the line charging of the shunt elements in the OPF formulation may result in significant deviations in the reactive powers of the network. Hence, in both Fig. 4 and Fig. 5, higher deviations in reactive power flows as compared to active power flows are obtained for the models neglecting line shunts (i.e., LinDF and DF). For reactive power injections, average deviations of 14.14%, 14.53%, 0.19% and 0.16% for the LinDF, DF, ExDF and ExAgDF models, respectively are obtained. The average deviations for different variables are summarized in Table I. Note that the inaccurate modeling of the lines can present major effects to the reactive power control of the network.

In this study, all models indicated no constraint violation for the voltage and line thermal limits. The different approximations and relaxations were thus able to provide an AC feasible solution in each case. However, uncertainties and variations in operational conditions may lead to deviations from reported results. We further compared the computational performance of the different models to access their practical application.

3) Computational Performance: In Table I, the operational costs and computational times of the different models are compared. The LinDF model as a linear approximation of the AC power flow indicated the fastest time and a low cost. Note however that this model provides an optimistic solution for the OPF problem. The ExAgDF provided the lowest optimal cost but the solution time in comparison
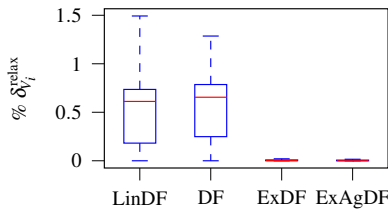
Fig. 3. Voltage deviations of the different relaxations to the local solution of the NLP model.
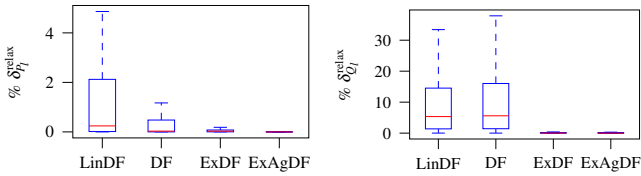

Fig. 4. Power flow deviations of the different relaxations to the local solution of the NLP model.

TABLE I
COMPUTATION TIME, OPTIMAL COST AND AVERAGE VARIATIONS OF THE DIFFERENT ALGORITHMS

	NLP	LinDF	DF	ExDF	ExAgDF
Comput. Time [s]	727.34	0.18	2.04	2.86	171.52
Total Cost [$]	38133	39088	41155	38122	38080
% $\delta_{V_i}^{\text{relax}}$	-	0.52	0.57	0.005	0.003
% $\delta_{p_i}^{\text{relax}}$	-	7.54	3.19	0.24	0.03
% $\delta_{q_i}^{\text{relax}}$	-	23.60	23.65	0.33	0.31
% $\delta_{P_l}^{\text{relax}}$	-	6.69	4.23	0.20	0.03
% $\delta_{Q_l}^{\text{relax}}$	-	14.14	14.58	0.19	0.16

with the other relaxations is relatively high. It is worthwhile to mention that the auxiliary variables used in the augmentations of this model while ensuring AC feasibility and greater accuracy result in a larger solution space that increases the computational time of the model. The NLP model guarantees AC feasibility but only provides a locally optimum solution. However, as detailed in Table I, this model suffers from a large computational time in comparison with the approximated and relaxed models and can fail to converge in some instances. The choice between accuracy in network modeling and computation performance will thus dictate the end application of the model. For larger networks, the computational performance of the LinDF model can provide a faster solution at a cost of lower accuracy and optimality.

V. CONCLUSION

The OPF solution provides a fundamental result for network analysis. We have compared five models that can practically be applied in the study of LVDNs using different metrics for a multi-period formulation. The optimality gap while providing an indication of the quality of the objective value may not provide a detailed indication of feasibility of
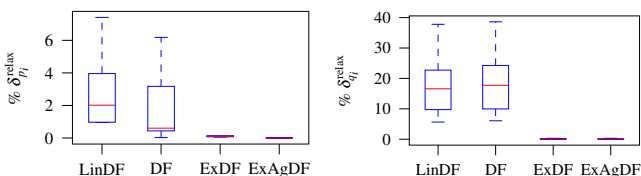

Fig. 5. Power injection deviations of the different relaxations to the local solution of the NLP model.

a linearization or relaxation. Using average deviations of different OPF variables, we were able to obtain the divergence of each variable from local optimality and an indication of the AC feasibility of the approximation/relaxation. We further investigated the effect of accurate network modeling to the OPF solution by analyzing the results of approximations and relaxations with/without line shunts. The results of approximated/relaxed models highlight significant effects of ignoring shunt elements to reactive power control. Finally, we analyzed the computational performance of each model to evaluate their scalability for the larger networks. Future works will further apply the OPF models that include the line shunts for voltage and reactive power control in distribution networks. Additionally, this models will be enhanced to handle uncertain variations in the network using a robust reformulation.

REFERENCES

[1] J. Carpentier, "Contribution to the economic dispatch problem," *Bull. Soc. Fr. Electr*, vol. 3, no. 8, 1962.

[2] D. K. Molzahn and I. A. Hiskens, *A Survey of Relaxations and Approximations of the Power Flow Equations.* Foundations and Trends® in Electric Energy System, 2019, vol. 4, no. 1-2.

[3] A. Venzke, S. Chatzivasileiadis, and D. K. Molzahn, "Inexact convex relaxations for ac optimal power flow: Towards ac feasibility," *Electric Power Systems Research*, vol. 187, p. 106480, 2020.

[4] P. Panciatici, M. C. Campi, S. Garatti, S. H. Low, D. K. Molzahn, A. X. Sun, and L. Wehenkel, "Advanced optimization methods for power systems," in *2014 Power Sys. Compn. Conf.*, 2014, pp. 1–18.

[5] J. Lavaei and S. H. Low, "Zero duality gap in optimal power flow problem," *IEEE Transactions on Power Systems*, vol. 27, no. 1, pp. 92–107, 2012.

[6] K. Christakou, D.-C. Tomozei, J.-Y. Le Boudec, and M. Paolone, "Ac opf in radial distribution networks – part i: On the limits of the branch flow convexification and the alternating direction method of multipliers," *Electric Power Systems Research*, vol. 143, pp. 438–450, 2017.

[7] F. Zhou and S. H. Low, "A note on branch flow models with line shunts," *IEEE Trans. on Pow. Sys.*, vol. 36, no. 1, pp. 537–540, 2021.

[8] M. Nick, R. Cherkaoui, J. L. Boudec, and M. Paolone, "An exact convex formulation of the optimal power flow in radial distribution networks including transverse components," *IEEE Trans. on Automatic Control*, vol. 63, no. 3, pp. 682–697, 2018.

[9] M. E. Baran and F. F. Wu, "Network reconfiguration in distribution systems for loss reduction and load balancing," *IEEE Trans. on Pow. Delivery*, vol. 4, no. 2, pp. 1401–1407, 1989.

[10] S. H. Low, "Convex relaxation of optimal power flow—part ii: Exactness," *IEEE Trans. on Control of Net. Sys.*, vol. 1, no. 2, pp. 177–189, 2014.

[11] M. Farivar and S. H. Low, "Branch flow model: Relaxations and convexification—part i," *IEEE Trans. on Pow. Sys.*, vol. 28, no. 3, pp. 2554–2564, 2013.

[12] Z. Yang, H. Zhong, A. Bose, T. Zheng, Q. Xia, and C. Kang, "A linearized opf model with reactive power and voltage magnitude: A pathway to improve the mw-only dc opf," *IEEE Trans. on Pow. Sys.*, vol. 33, no. 2, pp. 1734–1745, 2018.

[13] W. H. Kersting, "Radial distribution test feeders," in *2001 IEEE Pow. Eng. Soc. Winter Meeting. Conf. Proc. (Cat. No.01CH37194)*, vol. 2, 2001, pp. 908–912 vol.2.

[14] N. Blair, N. DiOrio, J. Freeman, P. Gilman, S. Janzou, T. Neises, and M. Wagner, "System Advisor Model (SAM) General Description (Version 2017.9.5)," National Renewable Energy Laboratory, Golden, CO, Tech. Rep. NREL/ TP-6A20-70414, May 2018.

[15] W. E. Hart, J.-P. Watson, and D. L. Woodruff, "Pyomo: modeling and solving mathematical programs in python," *Mathematical Programming Computation*, vol. 3, no. 3, pp. 219–260, 2011.

[16] Gurobi Optimization, LLC, "Gurobi optimizer reference manual," 2020. [Online]. Available: http://www.gurobi.com

[17] A. Wächter and L. T. Biegler, "On the implementation of an interior-point filter line-search algorithm for large-scale nonlinear programming." *Math. Program.*, vol. 106, p. 25–57, 2007.